HHS Public Access

Author manuscript

J Control Release. Author manuscript; available in PMC 2022 September 21.

Published in final edited form as:

J Control Release. 2022 September ; 349: 929–939. doi:10.1016/j.jconrel.2022.07.042.

Camptothesome Elicits Immunogenic Cell Death to Boost Colorectal Cancer Immune Checkpoint Blockade

Zhiren Wang[1], **Wenpan Li**[1], **Jonghan Park**[1], **Karina Marie Gonzalez**[1], **Aaron James Scott**[2,3], **Jianqin Lu**[1,2,4,5]

[1]Skaggs Pharmaceutical Sciences Center, Department of Pharmacology & Toxicology, R. Ken Coit College of Pharmacy, The University of Arizona, Tucson, Arizona, 85721, United States

[2]NCI-designated University of Arizona Comprehensive Cancer Center, Tucson, Arizona, 85721, United States

[3]Division of Hematology and Oncology, Department of Medicine, College of Medicine, The University of Arizona, Tucson, Arizona, 85721, United States

[4]BIO5 Institute, The University of Arizona, Tucson, Arizona, 85721, United States

[5]Southwest Environmental Health Sciences Center, The University of Arizona, Tucson, 85721, United States

Abstract

Camptothesome is an innovative nanovesicle therapeutic comprising the sphingomyelin-derived camptothecin (CPT) lipid bilayer. In this work, we deciphered that Camptothesome was taken up by colorectal cancer (CRC) cells through primarily the clathrin-mediated endocytotic pathway and displayed the potential of eliciting robust immunogenic cancer cell death (ICD) via upregulating calreticulin, high mobility group box 1 protein (HMGB-1), and adenosine triphosphate (ATP), three hallmarks involved in the induction of ICD. In addition, use of dying MC38 tumor cells treated with Camptothesome as vaccine prevented tumor growth in 60 % mice that received subsequent injection of live MC38 cells on the contralateral flank, validating Camptothesome was a legitimate ICD inducer *in vivo*. Camptothesome markedly reduced the acute bone marrow toxicity and gastrointestinal mucositis associated with free CPT and beat free CPT and Onivyde on anti-CRC efficacy and immune responses in a partially interferon gamma (IFN-γ)-dependent manner. Furthermore, Camptothesome enhanced the efficacy of immune checkpoint inhibitors to shrink late-stage orthotopic MC38 CRC tumors with diminished tumor metastasis and markedly prolonged mice survival.

Address correspondence to: Jianqin Lu, B.Pharm., Ph.D., Assistant Professor & Director, Pharmaceutics & Pharmacokinetics Track, Skaggs Pharmaceutical Sciences Center 422, Department of Pharmacology & Toxicology, R. Ken Coit College of Pharmacy, The University of Arizona, 1703 East Mabel Street, Tucson, AZ 85721, Tel: 520-626-1786; Fax: 520-626-2466, lu6@pharmacy.arizona.edu.

Declaration of competing interest

J.L. has applied for patents related to Camptothesome technology. The other authors have no competing interests.

Credit author statement

Jianqin Lu: Conceptualization; Supervision; Formal analysis; Writing – original draft; Funding acquisition. Zhiren Wang: Conceptualization; Methodology, Formal analysis, Investigation, Writing – original draft, Visualization. Wenpan Li: Investigation. Jonghan Park: Investigation. Karina Marie Gonzalez: Investigation. Aaron James Scott: Conceptualization.

Keywords

Camptothecin; Camptothesome; Clathrin-mediated endocytosis; Immunogenic cell death; Metastatic colorectal cancer; Immune checkpoint blockade

1. Introduction

CPT, a natural occurring pentacyclic alkaloid, was isolated from the stem wood of Chinese tree Camptotheca acuminata and has shown a wide range of anticancer activity (e.g., CRC) in preliminary clinical trials through inhibiting the topoisomerase I enzyme during the DNA replication, leading to strand breaks and subsequent apoptosis[1]. Nevertheless, its low aqueous solubility and debilitating systemic toxicities greatly hindered its therapeutic application and resulted in disappointing efficacy in clinical trials[2–4]. To circumvent these limitations, extensive efforts have been on developing water-soluble CPT analogues (irinotecan, topotecan, belotecan, etc). While these CPT derivatives addressed the solubility issue, the antineoplastic activity was drastically decreased and major toxicities associated with CPT such as gastrointestinal (GI) tract abnormalities (e.g., mucositis) and bone marrow toxicity (e.g., myelosuppression) remain unresolved.[5–9] Thus, there is an urgent need for the improved therapeutic delivery of CPT[10–12].

Unlike normal apoptosis, which is mostly nonimmunogenic or even tolerogenic, immunogenic cancer cell death (ICD) can induce an effective antitumour immune response through activation of antigen-presenting cells (e.g., dendritic cells, DCs) and consequent stimulation of cytotoxic T lymphocytes (CTLs) immunity[13, 14]. This ICD process was initiated by the translocation of calreticulin (“eat-me” signal for DC uptake) from endoplasm to the cell surface with concurrent release of HMGB-1 and ATP (adjuvant stimuli to DCs). Recent studies demonstrated that select chemotherapeutic agents, radiation, and photodynamic therapy are able to induce the ICD in cancers[15–21].

Previously, we developed a Camptothesome nanotherapeutic platform, which comprises Sphingomyelin (SM)-derived CPT lipid bilayer[22]. SM is a natural phospholipid existent in mammalian cell membrane[23] and has been approved by United States Food and Drug Administration (FDA) as the backbone lipid component used in liposomal nanotherapeutic, Marqibo[24]. Camptothesome readily addressed the solubility of CPT by forming nanovesicles in aqueous medium, and improved the pharmacokinetics and tumor delivery efficiency of CPT, as well as preserved the bilayer integrity, which would otherwise be compromised if CPT was entrapped in the lipid membrane physically. Compared to the low drug loading capacity (DLC, < 0.15% CPT) by conventional liposomes[22, 25], Camptothesome markedly increased the DLC to 6.1% with good stability[22].

Herein, using different endocytic pathway inhibitors, we elucidated that Camptothesome was internalized by CT26 and MC38 CRC cells chiefly via the clathrin-mediated endocytosis and dramatically reduced GI mucositis and acute bone marrow toxicity associated with free CPT at the maximum tolerated dose (MTD). Camptothesome was proven to be robust ICD inducer because it markedly increased the calreticulin expression on the cell surface and enhanced the release of HMGB-1 and ATP; and the dying MC38 cancer

cells treated by it as vaccine successfully prevented a large portion of the subsequent tumor development following the inoculation of the live MC38 tumor cells on the contralateral side of mice. Further, we deciphered that at the equivalent CPT dose, Camptothesome outperformed free CPT and Onivyde on therapeutic efficacy and CTL immunity, which was partially IFN-γ dependent. Notably, Camptothesome potentiated the immune checkpoint blockade therapy, resulting in tumor shrinkage and minimized metastasis in late-stage metastatic orthotopic MC38 tumor mouse model.

2. Materials and methods

The preparation of Camptothesome and Cy5.5/Camptothesome nanovesicles

The SM-CSS-CPT was synthesized, and Camptothesome and Cy5.5/Camptothesome nanovesicles were prepared by standard thin-film hydration approach. Camptothesome with 6.1% of CPT DLC was prepared as published[22] and used in this study. DLC was calculated as following[22]:

$$= \frac{\text{weight of conjugated CPT in Camptothesome}}{\text{weight of Camptothesome}} \times 100\% \qquad \text{equation (1)}$$

Cells and mice

The CT26 cell line was obtained from UArizona Cancer Center and cultured in complete RPMI-1640 medium. MC38 cell line was purchased from Kerafast and cultured in complete DMEM medium. The cells were cultured in the corresponding medium containing 10% FBS, 100 U/mL penicillin, 100 μg/mL streptomycin, and 2 mM L-glutamine at 37 °C with a CO_2 incubator. C57BL/6 mice (Charles Rivers, ~6 weeks old, female) were used. Tumor size was monitored by a digital caliper at indicated times and calculated using the formula=0.5 × length × width^2. Mice were euthanized and removed from the respective study when individual tumor reached ~2000 mm^3 in size or animals became moribund with severe weight loss, extreme weakness, or inactivity. The animals were maintained under pathogen-free conditions and all animal experiments were approved by the UArizona Institutional Animal Care and Use Committee (IACUC).

Apoptosis and necrosis study

1×10^5 MC38 or CT26 cells were seeded in 12-well plates and incubated overnight. The cell culture medium was removed and replenished with free CPT, Onivyde or Camptothesome containing media at the equivalent 1 μM or 5 μM of CPT for 20 h. Cells were trypsinized and washed with cold PBS first, then stained by using the FITC Annexin V apoptosis detection kit (BD Pharmingen™, #51-65874X) and PI (BD Pharmingen™, #51-66211E) according to the manufacturer's protocol. Cells were then measured by a flow cytometeter (BD FACSCanto II, BD Bioscience) and the data were analyzed by FlowJo software (version 10.0.7, TreeStar). The numbers presented in the flow cytometry plots were percentage based.

ICD biomarkers analysis

A total of 1×10^5 CT26 or MC38 cells were plated in 12-well plates. After 12 h, the cell culture medium was removed and replenished with free CPT, Onivyde or Camptothesome containing media at the 1 μM or 5 μM (CPT or Onivyde) for 20 h. Supernatants were collected to measure the released HMGB-1 or ATP concentrations by using an HMGB-1 ELISA kit (IBL International GmbH, #ABIN6574155) or ATPlite one-step luminescence assay kits (PerkinElmer, #6016736) following the manufacturers' instructions, respectively. To determine the cellular surface calreticulin expression by flow cytometry, cells were trypsinized and washed with cold PBS first, then stained with an Alexa Fluor® 647-conjugated anti-calreticulin antibody (Abcam, ab196159, 1/500) in staining buffer (eBioscience, #00-4222-26) at 4 °C for 30 min. After being washed with PBS (4 °C) twice, the cells were suspended in 400 μL of staining buffer and analyzed by a BD FACSCanto™ II flow cytometer (BD Bioscience). The data were presented as fold-increase in mean positive percentage ratio compared to the no treatment control group.

Vaccination experiment

MC38 cells were treated with free CPT, Onivyde or Camptothesome at equivalent 5 μM CPT for 20 h. Afterwards, 1×10^6 dying MC38 cells in 100 μL PBS (4 °C) were subcutaneously inoculated twice into the left flank of C57BL/6 mice (n = 5) at an interval of 7 days. Control group mice were injected with 5% Dextrose. 7 days after the 2nd inoculation, 1×10^5 live MC38 cells in 100 μL of serum free medium were subcutaneously injected into the right flank of the mice. Mice were photographed on day 25; tumor growth, mice body weight and survival were closely monitored as indicated.

Intracellular uptake mechanism of Camptothesome

To explore the potential mechanism involved in the cellular uptake process, 1×10^5 MC38 or CT26 cells were seeded in 12-well plates and incubated overnight. The medium was then replenished with fresh medium containing respective endocytosis inhibitors: [11] chlorpromazine (50 μM, clathrin-mediated endocytosis inhibitor), genistein (200 μM, caveolae-mediated endocytosis inhibitor), methyl-β-cyclodextrin (Me-β-CD, 800 μM, caveolae-mediated endocytosis inhibitor), wortmannin (5 μM, macropinocytosis inhibitor), cytochalasin D (5 μM, macropinocytosis inhibitor), or NaN_3 (10 mM, energy-dependent endocytosis inhibitor) for 30 min before being treated with Cy5.5/Camptothesome (50 μg CPT/mL) for 2 h at 37 °C. In another independent assay, cells were only treated with Cy5.5/Camptothesome at 4 °C or 37 °C for 2 h, respectively. Finally, the cells were trypsinized, washed with cold PBS twice, then resuspended in 400 μL of staining buffer (eBioscience, #00-4222-26) and analyzed by a BD FACSCanto™ II flow cytometer (BD Bioscience).

GI tract and bone marrow toxicity assessment.

Healthy BALB/c mice (n=3) were intravenously injected with the maximum tolerated dose (MTD) of free CPT (5 mg/kg), or Camptothesome (30 mg CPT/kg), respectively[22]. All the mice were sacrificed 7 days after the drug administration; blood, sternum and intestine were collected for analysis of citrulline levels, haematoxylin & eosin (H&E) staining, and periodic acidSchiff (PAS) reaction and counterstained with haematoxylin,

respectively. The mean number of PAS^+ goblet cells per crypt column in the intestine was statistically analysed by one-way ANOVA to assess the mucositis in GI tract[26]. For citrulline measurement, blood was collected in lithium heparin tubes (BD Microtainer™). After centrifuging at 2,000 g for 10 minutes in a refrigerated centrifuge, the supernatant (serum) was meticulously collected and directly measured by the citrulline assay kit (Abcam, #ab242292) according to the manufacturer's protocol. To evaluate the bone marrow and hematopoietic cellularity in the sternums, H&E staining of sternums was analyzed by Aperio ImageScope software (version 12.4.3.5008)[27].

Therapeutic efficacy study

In subcutaneous MC38 tumor-bearing mice—MC38 cells (1×10^5) in 100 μL of serum free medium were subcutaneously injected to the C57BL/6 mice (n=5).

In Fig. 4, when tumors grew to ~100 mm^3 in size on day 12, mice received a single intravenous injection of 5% Dextrose (vehicle control), free CPT, Onivyde (8.4 mg irinotecan/kg) or Camptothesome at equivalent 5 mg CPT/kg. Mice were photographed on day 21, and tumors were isolated and divided into 3 pieces for flow cytometry, ELISA and western blotting analysis as described below, respectively..

In Fig. 5, when tumors reached ~200 mm^3 on day 15, mice were intravenously injected once with Camptothesome (20 mg CPT/kg) or in combination with α-IFN-γ (BioXcell, clone R4-6A2, 200 μg/mouse/3 days, intraperitoneally administered)[28]. Mice were photographed on day 22, and tumors were isolated for flow cytometry analysis as described below.

In orthotopic MC38 tumor-bearing mice—C57BL/6 mice were initially anesthetized with isoflurane, and a shaver was used to remove the hair/fur in abdominal area. Then three alternating scrubs of betadine/povidone iodine followed by 70% ethanol were applied to the surgical area. Before the surgery, mice were subcutaneously injected with buprenorphine HCl (0.5 mg/kg). Whereafter, an abdominal incision (~1 cm) was made by using a sterile disposable scalpel, and the caecum was exteriorized. By using a 26-gauge needle (BD precisionGlide™), 2×10^6 MC38 cells in 50 μL of DMEM medium with Matrigel (Corning, Discovery labware Inc.) (3/1, v/v) were inoculated into the caecum subserosa. Afterwards, caecum was replaced into the peritoneal cavity after the injection site was sterilized with 70% ethanol to kill cancer cells that may have leaked out. The abdominal wall and skin were sutured by size 6–0 absorbable sutures (PDS II, Ethicon) and size 5–0 nonabsorbable sutures (PROLENE, Ethicon), respectively. Surgical glue was applied to ensure good apposition of the skin. Mice were placed on the heating pad during and after surgery and closely monitored until ambulatory, then placed back to a clean cage. 12 days after MC38 cells inoculation (primary tumor weight: ~400 mg, ~30–40% of mice successfully developed tumor). Orthotopic MC38 tumor-bearing C57BL/6 mice were randomly allocated into 6 groups (n=5 mice). Mice were then intravenously administered with a single dose of Camptothesome or Onivyde (33.6 mg irinotecan/kg) at equivalent 20 mg CPT/kg, or their combination with α-PD-L1 + α-PD-1. α-PD-L1 (BioXCell, clone 10F.9G2) and α-PD-1 (BioXCell, clone RMP1–14) were intraperitonerally administered at 100 μg/mouse/3 days

for 3 times[29]. 5% Dextrose and α-PD-L1 + α-PD-1 were control groups. On day 24, mice were dissected, and gastrointestinal tract and other major organs (heart, liver, spleen, lung, kidneys, stomach, small and large intestines, cecum and rectum) were quickly obtained and then photographed to investigate the tumor metastasis. The primary tumors were weighed by a digital balance (SHIMADZU, AUW220D). A parallel efficacy study (n=6 mice) was conducted to evaluate the mouse survival.

Flow cytometry analysis

Tumors collected from mice were divided into small pieces by scissors and digested in DMEM containing 0.5 mg/mL collagenase type I (Worthington Biochemical Corporation, NC9482366) at 37 °C for 1 h. Afterwards, the digested tissues were meshed through a 70 μM cell strainer for two times. Ack lysing buffer (Gibco, #2217610) was used to lyse the red blood cells based on the manufacturer's protocols. Then, the cell suspensions were washed with 4 °C PBS twice and resuspended in 4 °C staining buffer (eBioscience, #00-4222-26). After counting and aliquoting the cells, the cell suspensions were pre-incubated with FcBlock (TruStain fcXTM anti-mouse CD16/32, clone 93, 101320, BioLegend, 0.5 μg/100 μL) for 20 min at 4 °C to avoid nonspecific binding. Cells were then stained with various combinations of fluorophore-labeled antibodies for 30 min at 4 °C. CD45-APC-Cy™7 (30-F11, #557659, 1/100), CD8a-PE (53–6.7, #561095, 1/100), CD11c-V450 (HL3, #560521, 1/100), CD80-APC (16-10A1, #553766, 1/100), CD86-PE (GL1, #553692,1/100) were purchased from BD Biosceinces. Granzyme B eFluor 660 (NGZB, #50-8898-82, 1/100) were purchased from eBiosciences. IFN-γ-APC (XMG1.2, #505810, 1/100) was purchased from BioLegend. CD3-APC-eFluor 780 (17A2, #47-0032-82, 1/100) was purchased from Invitrogen. Multi-parameter staining was utilized to measure the following cell populations: (i) IFN-γ^+ T cells ($CD3^+/CD8^+/IFN\text{-}\gamma^+$), (ii) granzyme B^+ T cells ($CD3^+/CD8^+$/granzyme B^+), (iii) $CD80^+/CD86^+$ DCs ($CD45^+/CD11c^+/CD80^+/CD86^+$). For IFN-γ staining, cells were treated with a cell stimulation cocktail (eBioscience, #00-4975-93) for 4 h prior to extracellular and intracellular staining according to the manufacture's protocol. Cells were fixed and permeabilized using a staining Buffer Set (eBioscience, #00-5523-00) followed by intracellular staining of IFN-γ or granzyme B. Post washing, cells were then measured by a flow cytometeter (BD FACSCanto II, BD Bioscience) and the data were analyzed by FlowJo software (version 10.0.7, TreeStar). The numbers presented in the flow cytometry plots were percentage based.

ELISA test

The tumor tissues were thawed at room temperature and homogenized by bead beating in PBS (1 mL PBS/100 mg tissue) at 4 °C. After centrifuging at a speed of 15000 rpm/min for 10 min, the supernatants were collected for ELISA tests[30]. The procedures were followed the manufacturer's instructions of TNF-α (Invitrogen, #KHC3011), IL-6 (Abcam, ab222503), IFN-β (Bio-techne, #42400-1) and IFN-γ (LSBio, LS-F3414) ELISA kits.

Western blotting

The tumor tissues were homogenized by bead beating in RIPA buffer containing with 1% proteinase inhibitor cocktail (200 μL/20 mg tissue, ThermoFisher, #78429) within 10 min at 4 °C. The lysates were then centrifuged at 15,000 r.p.m. for 20 min at 4 °C, the supernatants

were collected and quantified by BCA assay. Samples were dissolved in SDS-PAGE protein loading buffer (5X, Boster, AR1112) and boiled for 10 min, and equal amounts of each sample were applied to 12% Tris-glycine gel (Novex gel, Invitrogen) and subjected to electrophoresis, which was subsequently transferred to a PDVF (polyvinylidene difluoride) membrane and blocked in 5% non-fat milk blocking buffer for 1 h at room temperature. The membranes were incubation with the primary antibody overnight at 4 °C (STING (D1V5L) mAb, #50494, dilution 1/1000; Phospho-STING (Ser365) (D8F4W) mAb, #72971, dilution 1/1000; IRF-3 (D83B9) mAb, #4302, dilution 1/1000; Phospho-IRF-3 (Ser396) (D6O1M) mAb, #29047, dilution 1/1000, Cell Signaling; β-Actin, ab179467, dilution 1/1000, Abcam), and then horseradish peroxidase (HRP)-conjugated secondary antibodies (anti-rabbit IgG, HRP-linked antibody, #7074, dilution 1/3000; Cell Signaling). Finally, the membranes were soaked in ECL substrate (Thermo Scientific) and imaged under Azure Biosystems software (v. 1.5.0.0518).

3. Results and discussion

3.1 Cellular uptake mechanism of Camptothesome

To decipher if the intracellular internalization of Camptothesome is via endocytosis, we first evaluated the impact of temperature dependence (4 °C vs 37 °C) on uptake in CT26 CRC cells (Fig. 1c). Cy5.5-labeled Camptothesome were synthesized as previously established[22]. Flow cytometry analysis revealed that the cellular uptake of Cy5.5/Camptothesome was almost completely inhibited (~98%) at 4 °C in comparison to the vehicle control group (5% Dextrose, 37 °C); and NaN_3 pretreatment also resulted in significant uptake suppression (~57%), demonstrating an energy-dependent cellular internalization mechanism. These findings are in line with the report that endocytic/pinocytic uptake was deactivated at 4 °C[31]. To dive deeper into the underlying cellular uptake mechanism that Camptothesome may utilize to enter cells, CT26 cells were pre-treated with various endocytotic inhibitors. We showed that cellular uptake of Cy5.5/Camptothesome was almost not affected by the caveolae-mediated endocytotic inhibitors (genistein and methyl-β-cyclodextrin) and was only partially (~21 or ~20%) impeded by the macropinocytosis inhibitors (wortmannin and cytochalasin D). Nonetheless, clathrin-mediated endocytosis inhibitors (chlorpromazine) substantially reduced cellular uptake level by ~78%. These results suggested that Cy5.5/Camptothesome was ingested by CT26 cells primarily through clathrin-mediated endocytosis, despite the minor role of macropinocytosis. The clathrin-mediated endocytotic cellular uptake mechanism can allow Camptothesome to bypass the P-glycoprotein-mediated efflux pump that is frequently upregulated in tumors[32–35], thereby potentially overcoming the multidrug resistance and improving therapeutic effects[36, 37]. These results were confirmed in MC38 CRC cells (Supplementary Fig. 1).

3.2 Camptothesome instigates ICD immune response in CRC

To evaluate the cytotoxicity of Camptothesome, the cell apoptosis and necrosis were investigated by FITC Annexin V and propidium iodide (PI) using flow cytometry (Fig. 2a,b). Camptothesome induced 20.4% necrotic/late apoptotic cells (Annexin V^+ PI^+) and 4.5% early apoptotic (Annexin V^+ PI^-) at 1 μM, which were further increased to 35.0% and

9.5% at 5 μM, respectively. Similar trends were also observed in CT26 cells (Supplemental Fig. 2). During ICD, calreticulin serves as the “eat-me” signal for the dying tumor cells uptake by antigen-presenting DCs, with accompanying release of adjuvant stimuli, HMGB-1 and ATP to boost the DCs maturation and cross-presentation of endogenous tumor associated antigens, which aggregately will recruit and activate CTLs to elicit killing for both primary and metastatic cancer cells[15, 38, 39]. Thus, to evaluate the ICD response induced by Camptothesome, the calreticulin expression in MC38 and CT26 cell was first analyzed by flow cytometry. Onivyde, the FDA-approved liposomal irinotecan (a CPT analog), showed negligible calreticulin induction on MC38 cells when compared to the no treatment control. In contrast, free CPT treatment was able to markedly increase the calreticulin expression on MC38 cells in a dose-dependent manner (Fig. 2c,d). This can be ascribed to the weaker in vitro cancer cells-killing activity of Onivyde as compared to free CPT[40, 41]. Of note, at the equivalent CPT dose, Camptothesome further fortified the expression of calreticulin on MC38 cells, which was 2.1-fold or 3.4-fold more than that of Onivyde at 1 μM or 5 μM, respectively (Fig. 2c,d). Interestingly, Camptothesome also enhanced the HMGB-1 and ATP release (Fig. 2e,f). To rule out these effects are not cell line-dependent, we performed the calreticulin, HMGB-1 and ATP assays in CT26 cells and similar results were obtained (Supplemental Fig. 2).

To further substantiate the ICD potential of Camptothesome *in vivo*, a standard vaccination experiment was performed in immune competent C57BL/6 mice. Dying MC38 cells were produced by free CPT, Onivyde, or Camptothesome treatment at equivalent 5 μM CPT for 20 h. Mice were then injected subcutaneously by two times of dying MC38 cells (one week apart) and were subsequently challenged with live MC38 cells on the contralateral flank (Fig. 2g). Vaccination using Onivyde-treated cells did not prevent the tumor growth on the contralateral side of mice; however, vaccination with free CPT-treated cells significantly inhibited contralateral tumor development and completely prevented 1 out of 5 mice to grow tumor (Fig. 2h–j). Strikingly, Camptothesome-treated cells vaccine further boosted the tumor suppression and prolonged the mice survival with 3 out of 5 mice survived tumor-free (Fig. 2h–j). The tumor cells treated with Camptothesome worked better as a vaccine than the cells treated with free CPT could be due to the fortified ICD effect as manifested by the increased levels of calreticulin, HMGB-1 and ATP triggered by Camptothesome. Taken together, our *in vitro* and *in vivo* studies verified that Camptothesome is a robust ICD inducer in CRC.

3.3 Camptothesome reduces the GI mucositis and bone marrow damage

The major systemic toxicities associated with CPT are GI toxicities and myelosuppression[8, 9]. To find out whether Camptothesome can alleviate these adverse effects, we evaluated the blood citrulline, a biomarker for GI mucositis frequently induced by chemotherapy[43] and the intestinal mucosa using periodic acid-Schiff (PAS) reaction[26], as well as the bone marrow using H&E staining in mice treated with a single intravenous MTD for free CPT (5 mg/kg), or Camptothesome (30 mg CPT/kg)[22]. 7 days after treatments, PAS reaction was performed for examining the intestinal mucositis, and the blood was withdrawn for the analysis of citrulline levels (Fig 3a–c). We revealed that free CPT at MTD markedly induced hyperplasia and enlargement of mucin-containing goblet

cells in the crypt column of intestines as compared to that of vehicle control (5% dextrose), indicative of GI mucositis[44, 45]; In contrast, Camptothesome at MTD did not trigger these untoward effects by controlling the number of PAS^+ mucin-containing goblet cells without morphological enlargement (Fig 3a,b). In addition, while MTD of Camptothesome allowed blood citrulline remain at the similar level as that of vehicle control, free CPT MTD significantly attenuated the blood citrulline levels as compared to the vehicle control (Fig 3c). Meanwhile, the sternum tissues were collected from the MTD mice to investigate the acute bone marrow toxicity through H&E staining (Fig. 3d)[27, 46]. Our results showed that both the total bone marrow cellularity and nucleated hematopoietic cells in the sternums were dramatically decreased by free CPT (Fig. 3d–f), signifying considerable myelosuppressive effects. Notably, both types of cellularity in Camptothesome-treated group maintained at the consistent level as in that of 5% Dextrose. The reduced side effects of Camptothesome compared to free CPT could be attributed to 1) its less distribution to normal tissues[22]; and 2) controlled and minimized drug release kinetics during blood circulation and in healthy tissues[22, 47, 48]. All considered, these data demonstrated that Camptothesome can diminish the GI toxicity and myelosuppression associated with free CPT for safer clinical translation.

3.4 Camptothesome outperformes Onivyde on therapeutic efficacy and immunity in CRC mouse model

To demonstrate whether Camptothesome can improve the anti-CRC efficacy of CPT, we treated MC38 tumor (~100 mm^3)-bearing mice with one time of intravenous administration of free CPT or Camptothesome at the MTD of free CPT (equivalent 5 mg CPT/kg)[22]; Onivyde (8.4 mg irinotecan/kg, equivalent 5 mg CPT/kg) was used as the nanotherapeutic control (Fig. 4a,b). MC38 tumors in vehicle control grew rapidly, suggesting the aggressive nature of the tumor type. Free CPT treatment was able to significantly bring down the tumor development, which was enhanced by Onivyde, which could be attributed to the prolonged blood circulation time and enhanced tumor accumulation of Onivyde as compared to free CPT[22, 49, 50]. Interestingly, we showed that Camptothesome-mediated CPT delivery outperformed free CPT and Onivyde therapies on tumor reduction in a more pronounced manner (Fig. 4a,b). The better efficacy of Camptothesome may be credited to the improved PK and enhanced tumor delivery efficiency and effective release of CPT under the high intratumoral GSH concentration (~4–5 fold higher in tumors than normal tissues)[22, 47, 48]. While irinotecan was converted to its active metabolite form SN-38 by human carboxylesterase converting enzyme (CCE), which was 2–3 fold lower in tumors in comparison to normal tissues[51–53]. Then we asked if the fortified anticancer efficacy of Camptothesome was attributed to the increased antitumor immune responses. To answer this question, we evaluated the innate and adaptive immune actions triggered by Cmaptothesome. On day 21, the tumors from the MC38 mouse model were collected and processed for the flow cytometric analysis for examining the intratumoral $CD86^+/CD80^+$ DCs, granzyme $B^+/CD8^+$ T cells, as well as the IFN-$\gamma^+/CD8^+$ T cells populations (Fig. 4c–e). It has been reported that mature DCs can express high levels of CD80 and CD86, the two co-stimulatory molecules, providing indispensable signal for the T cell activation, expansion, and differentiation[13, 54]. Our multi-parameter flow cytometric staining ($CD45^+/CD11c^+/CD80^+/CD86^+$) demonstrated that free CPT only

marginally increased the mature DCs number. While Onivyde boosted the level of $CD80^+$/$CD86^+$ DCs, Camptothesome stimulated the maturation of DCs to the next extent (Fig. 4c). Given the innate immunity was activated by Camptothesome, then we proceeded to investigate the adaptive immune responses. IFN-γ is a pro-inflammatory cytokine that is critical for enhancing anti-tumor effects of $CD8^+$ T cells[13, 55]. Granzyme B is an essential mediator in $CD8^+$ T cell killing effects[13, 56]. We found that both the % of IFN-γ^+/$CD8^+$ T cells and Granzyme B^+/$CD8^+$ T cells were significantly elevated in the tumors treated with Camptothesome as compared to free CPT and Onivyde (Fig. 4d,e). To further probe whether Camptothesome can activate the STING pathway, first, we evaluated the proinflammatory cytokines (TNF-α, IL-6, IFN-β and IFN-γ) in tumors using ELISA assay[30]. Free CPT treatment had negligible effect on these cytokines. While Onivyde was able to markedly increase the levels of TNF-α, IL-6, IFN-β and IFN-γ, which were further significantly heightened by Camptothesome (Supplementary Fig. 3a). Moreover, Camptothesome enhanced phosphorylation of STING and IFN regulatory factor 3 (IRF3) inside the tumors in a way that is more significant than Onivyde. These data corroborated that the STING pathway was stimulated after the Camptothesome treatment (Supplementary Fig. 3b)[30]. Taken together, our results suggested that the activated CTLs and STING pathway in tumors may have contributed to the overall improved anti-CRC effects triggered by Camptothesome. To figure out the underlying mechanism of the antitumor immune responses elicited by Camptothesome, we systemically depleted IFN-γ in MC38 tumor model using the monoclonal antibody that reacts with mouse IFN-γ. Upon IFN-γ neutralization, the tumor inhibitory effect of Camptothesome was significantly attenuated as evidenced by the markedly bigger tumor size (Fig. 5a–c). Using flow cytometry, we found that the Camptothesome-induced IFN-γ^+/$CD8^+$ T cells and granzyme B^+/$CD8^+$ T cells in MC38 tumors were radically diminished when IFN-γ was knocked down systemically (Fig. 5d)[22, 28].

3.6 Camptothesome potentiates immune checkpoint blockade to shrink the late-stage orthotopic MC38 tumors with minimized metastasis

Late-stage metastatic orthotopic CRC tumors were considerably intractable and aggressive, and oftentimes result in despondent patient survival outcome in clinic. To investigate whether Camptothesome can favorably impact the more advanced CRC tumors, late-stage orthotopic MC38 tumor murine model with marked metastasis were established to mimic the clinically hard-to-treat CRC tumors. On day 12 post MC38 cells injection into the cecum subserosa, mice developed ~400 mg tumor blocks orthotopically with tumor metastatic nodules observed in other tissues (Fig. 6a,d), and mice were then intravenously administered by Onivyde or Camptothesome with or without antibodies targeting PD-L1/PD-1 immune checkpoints (α-PD-L1 + α-PD-1); 5% Dextrose and α-PD-L1 + α-PD-1 were used as controls. Mice were sacrificed on day 24 and photographs were taken to visualize the big tumor blocks as well as the metastatic tumor nodules (Fig. 6b,e). At the termination, vehicle control mice developed a considerable orthotopic tumor mass (~2.2 g) and had severe and widespread metastasis in liver, spleen, kidney, stomach, intestines, colon, and rectum. Co-blocking PD-L1 and PD-1 yielded negligible primary tumor reduction (tumors: ~1.9 g) and inappreciable metastasis alleviation, which substantiates that this advanced tumor model is poorly responsive to immune checkpoint blockade therapy (Fig. 6b–e,f). Onivyde

delivered appreciable inhibitory activity for orthotopic tumor growth (tumors: ~0.8 g), but merely reduced the metastasis in other organs/tissues. Combing with α-PD-L1 + α-PD-1 enhanced the efficacy of Onivyde to further reduce the primary tumor burden (tumors: ~0.6 g) and metastasis. Inspiringly, Camptothesome alone produced comparable therapeutic efficacy (tumors: ~0.4 g) as that of Onivyde plus α-PD-L1 + α-PD-1 combination therapy. Along with immune checkpoint inhibitors, Camptothesome can dramatically shrank primary tumors to ~35 mg with radically dampened tumor metastasis (Fig. 6b–e,f). Furthermore, a parallel efficacy study demonstrated that Camptothesome (MST=32.5) significantly prolonged the mice survival rate as compared with Onivyde (MST=28), which was drastically extended to another level (MST=51.5) when combined with α-PD-L1 + α-PD-1 (Fig. 6g). These findings confirmed that Camptothesome is superior to the clinically used nanotherapeutic, Onivyde in treating advanced metastatic CRC tumors, particularly in the context of combing with immune checkpoint inhibitors. The enhanced anti-CRC effects of Camptothesome can be attributable to its improved antitumor immunity through eliciting potent ICD and CTLs responses (Fig. 2,4).

4. Conclusions

In summary, we elucidated that Camptothesome was taken up by CRC cells mainly through the clathrin-mediated endocytosis. Via measuring calreticulin, HMGB-1, and ATP, as well as performing the vaccination experimentation, we confirmed that Camptothesome is a robust ICD inducer. At MTD, Camptothesome greatly dampened the GI toxicities and myelosuppression caused by free CPT. Camptothesome was superior to free CPT and Onivyde on suppressing the MC38 CRC tumor development as well as eliciting the anti-CRC immune responses, which was found to be partially IFN-γ dependent. Further, we showed that Camptothesome potentiated the efficacy of immune checkpoint blockade to entail the shrinkage of late-stage orthotopic MC38 tumors and minimize tumor metastasis with markedly prolonged mice survival rate. Our findings further corroborated that Camptothesome can be a safe and effective platform for the improved delivery of CPT to enhance the anticancer efficacy and immunity, as well as to bolster the responses of tumors to immune checkpoint blockade therapy.

Supplementary Material

Refer to Web version on PubMed Central for supplementary material.

Acknowledgements

This work was supported in part by a Startup Fund from the R. Ken Coit College of Pharmacy at The University of Arizona (UArizona) and a PhRMA Foundation for Research Starter Grant in Drug Delivery, and by National Institute of General Medical Sciences of the National Institutes of Health under Award Number R35GM147002. We acknowledge the Tissue Acquisition and Cellular/Molecular Analysis Shared Resource (TACMASR) at UArizona Cancer Center (UACC) for the histopathological staining.

Data availability

The data supporting the findings of this study are available within the article and the Supplementary Information. All relevant data are available from the authors upon reasonable request.

Reference

[1]. Schluep T, Hwang J, Cheng J, Heidel JD, Bartlett DW, Hollister B, Davis ME, Preclinical efficacy of the camptothecin-polymer conjugate IT-101 in multiple cancer models, Clin. Cancer Res, 12 (2006) 1606–1614. [PubMed: 16533788]

[2]. Creaven PJ, Allen LM, Muggia FM, Plasma camptothecin (NSC-100880) levels during a 5-day course of treatment: relation to dose and toxicity, Cancer Chemother. Rep, 56 (1972) 573–578. [PubMed: 4652588]

[3]. Muggia FM, Creaven PJ, Hansen HH, Cohen MH, Selawry OS, Phase I clinical trial of weekly and daily treatment with camptothecin (NSC-100880): correlation with preclinical studies, Cancer Chemother. Rep, 56 (1972) 515–521. [PubMed: 5081595]

[4]. Moertel CG, Schutt AJ, Reitemeier RJ, Hahn RG, Phase II study of camptothecin (NSC-100880) in the treatment of advanced gastrointestinal cancer, Cancer Chemother. Rep., 56 (1972) 95–101. [PubMed: 5030811]

[5]. Liu YQ, Li WQ, Morris-Natschke SL, Qian K, Yang L, Zhu GX, Wu XB, Chen AL, Zhang SY, Nan X, Lee KH, Perspectives on biologically active camptothecin derivatives, Med. Res. Rev, 35 (2015) 753–789. [PubMed: 25808858]

[6]. Caiolfa VR, Zamai M, Fiorino A, Frigerio E, Pellizzoni C, d'Argy R, Ghiglieri A, Castelli MG, Farao M, Pesenti E, Gigli M, Angelucci F, Suarato A, Polymer-bound camptothecin: initial biodistribution and antitumour activity studies, J. Controlled Release, 65 (2000) 105–119.

[7]. Venditto VJ, Simanek EE, Cancer therapies utilizing the camptothecins: a review of the in vivo literature, Mol Pharmaceut, 7 (2010) 307–349.

[8]. Hecht JR, Gastrointestinal toxicity or irinotecan, Oncology (Williston Park), 12 (1998) 72–78. [PubMed: 9726096]

[9]. Mathijssen RH, van Alphen RJ, Verweij J, Loos WJ, Nooter K, Stoter G, Sparreboom A, Clinical pharmacokinetics and metabolism of irinotecan (CPT-11), Clin. Cancer. Res, 7 (2001) 2182–2194. [PubMed: 11489791]

[10]. Shen S, Xu X, Lin S, Zhang Y, Liu H, Zhang C, Mo R, A nanotherapeutic strategy to overcome chemotherapeutic resistance of cancer stem-like cells, Nat. Nanotechnol., 16 (2021) 104–113. [PubMed: 33437035]

[11]. Zhou Q, Shao SQ, Wang JQ, Xu CH, Xiang JJ, Piao Y, Zhou ZX, Yu QS, Tang JB, Liu XR, Gan ZH, Mo R, Gu Z, Shen YQ, Enzyme-activatable polymer-drug conjugate augments tumour penetration and treatment efficacy, Nat. Nanotechnol, 14 (2019) 799–809. [PubMed: 31263194]

[12]. Guan J, Wu Y, Liu X, Wang H, Ye N, Li Z, Xiao C, Zhang Z, Li Z, Yang X, A novel prodrug and its nanoformulation suppress cancer stem cells by inducing immunogenic cell death and inhibiting indoleamine 2, 3-dioxygenase, Biomaterials, 279 (2021) 121180. [PubMed: 34768152]

[13]. Kroemer G, Galluzzi L, Kepp O, Zitvogel L, Immunogenic cell death in cancer therapy, Annu. Rev. Immunol, 31 (2013) 51–72. [PubMed: 23157435]

[14]. Green DR, Ferguson T, Zitvogel L, Kroemer G, Immunogenic and tolerogenic cell death, Nat. Rev. Immunol, 9 (2009) 353–363. [PubMed: 19365408]

[15]. Lu J, Liu X, Liao YP, Salazar F, Sun B, Jiang W, Chang CH, Jiang J, Wang X, Wu AM, Meng H, Nel AE, Nano-enabled pancreas cancer immunotherapy using immunogenic cell death and reversing immunosuppression, Nat. Commun, 8 (2017) 1811. [PubMed: 29180759]

[16]. Apetoh L, Ghiringhelli F, Tesniere A, Obeid M, Ortiz C, Criollo A, Mignot G, Maiuri MC, Ullrich E, Saulnier P, Yang H, Amigorena S, Ryffel B, Barrat FJ, Saftig P, Levi F, Lidereau R, Nogues C, Mira JP, Chompret A, Joulin V, Clavel-Chapelon F, Bourhis J, Andre F, Delaloge S, Tursz T, Kroemer G, Zitvogel L, Toll-like receptor 4-dependent contribution of the

immune system to anticancer chemotherapy and radiotherapy, Nat. Med., 13 (2007) 1050–1059. [PubMed: 17704786]

[17]. Casares N, Pequignot MO, Tesniere A, Ghiringhelli F, Roux S, Chaput N, Schmitt E, Hamai A, Hervas-Stubbs S, Obeid M, Coutant F, Metivier D, Pichard E, Aucouturier P, Pierron G, Garrido C, Zitvogel L, Kroemer G, Caspase-dependent immunogenicity of doxorubicin-induced tumor cell death, J. Exp. Med, 202 (2005) 1691–1701. [PubMed: 16365148]

[18]. Fucikova J, Kralikova P, Fialova A, Brtnicky T, Rob L, Bartunkova J, Spisek R, Human tumor cells killed by anthracyclines induce a tumor-specific immune response, Cancer Res, 71 (2011) 4821–4833. [PubMed: 21602432]

[19]. Michaud M, Martins I, Sukkurwala AQ, Adjemian S, Ma Y, Pellegatti P, Shen S, Kepp O, Scoazec M, Mignot G, Rello-Varona S, Tailler M, Menger L, Vacchelli E, Galluzzi L, Ghiringhelli F, di Virgilio F, Zitvogel L, Kroemer G, Autophagy-dependent anticancer immune responses induced by chemotherapeutic agents in mice, Science, 334 (2011) 1573–1577. [PubMed: 22174255]

[20]. Zappasodi R, Pupa SM, Ghedini GC, Bongarzone I, Magni M, Cabras AD, Colombo MP, Carlo-Stella C, Gianni AM, Di Nicola M, Improved clinical outcome in indolent B-cell lymphoma patients vaccinated with autologous tumor cells experiencing immunogenic death, Cancer research, 70 (2010) 9062–9072. [PubMed: 20884630]

[21]. Werthmoller N, Frey B, Wunderlich R, Fietkau R, Gaipl US, Modulation of radiochemoimmunotherapy-induced B16 melanoma cell death by the pan-caspase inhibitor zVAD-fmk induces anti-tumor immunity in a HMGB1-, nucleotide- and T-cell-dependent manner, Cell Death. Dis., 6 (2015) e1761. [PubMed: 25973681]

[22]. Wang Z, Little N, Chen J, Lambesis KT, Le KT, Han W, Scott AJ, Lu J, Immunogenic camptothesome nanovesicles comprising sphingomyelin-derived camptothecin bilayers for safe and synergistic cancer immunochemotherapy, Nat. Nanotechnol., 16 (2021) 1130–1140. [PubMed: 34385682]

[23]. Martinez-Beamonte R, Lou-Bonafonte JM, Martinez-Gracia MV, Osada J, Sphingomyelin in high-density lipoproteins: structural role and biological function, Int. J. Mol. Sci, 14 (2013) 7716–7741. [PubMed: 23571495]

[24]. Sedighi M, Sieber S, Rahimi F, Shahbazi MA, Rezayan AH, Huwyler J, Witzigmann D, Rapid optimization of liposome characteristics using a combined microfluidics and design-of-experiment approach, Drug Deliv. Transl. Res, 9 (2019) 404–413. [PubMed: 30306459]

[25]. Flaten GE, Chang TT, Phillips WT, Brandl M, Bao A, Goins B, Liposomal formulations of poorly soluble camptothecin: drug retention and biodistribution, J Liposome Res, 23 (2013) 70–81. [PubMed: 23210622]

[26]. Hardman WE, Moyer MP, Cameron IL, Fish oil supplementation enhanced CPT-11 (irinotecan) efficacy against MCF7 breast carcinoma xenografts and ameliorated intestinal side-effects, Br. J. Cancer, 81 (1999) 440–448. [PubMed: 10507768]

[27]. Travlos GS, Normal structure, function, and histology of the bone marrow, Toxicol. Pathol., 34 (2006) 548–565. [PubMed: 17067943]

[28]. Clemente-Casares X, Blanco J, Ambalavanan P, Yamanouchi J, Singha S, Fandos C, Tsai S, Wang J, Garabatos N, Izquierdo C, Agrawal S, Keough MB, Yong VW, James E, Moore A, Yang Y, Stratmann T, Serra P, Santamaria P, Expanding antigen-specific regulatory networks to treat autoimmunity, Nature, 530 (2016) 434–440. [PubMed: 26886799]

[29]. Song W, Shen L, Wang Y, Liu Q, Goodwin TJ, Li J, Dorosheva O, Liu T, Liu R, Huang L, Synergistic and low adverse effect cancer immunotherapy by immunogenic chemotherapy and locally expressed PD-L1 trap, Nat. Commun, 9 (2018) 2237. [PubMed: 29884866]

[30]. Zhao J, Ma S, Xu Y, Si X, Yao H, Huang Z, Zhang Y, Yu H, Tang Z, Song W, Chen X, In situ activation of STING pathway with polymeric SN38 for cancer chemoimmunotherapy, Biomaterials, 268 (2021) 120542. [PubMed: 33249316]

[31]. Tomoda H, Kishimoto Y, Lee YC, Temperature effect on endocytosis and exocytosis by rabbit alveolar macrophages, J. Biol. Chem, 264 (1989) 15445–15450. [PubMed: 2768271]

[32]. Ortiz R, Quinonero F, Garcia-Pinel B, Fuel M, Mesas C, Cabeza L, Melguizo C, Prados J, Nanomedicine to Overcome Multidrug Resistance Mechanisms in Colon and Pancreatic Cancer: Recent Progress, Cancers, 13 (2021).

[33]. Sivak L, Subr V, Tomala J, Rihova B, Strohalm J, Etrych T, Kovar M, Overcoming multidrug resistance via simultaneous delivery of cytostatic drug and P-glycoprotein inhibitor to cancer cells by HPMA copolymer conjugate, Biomaterials, 115 (2017) 65–80. [PubMed: 27886555]

[34]. Liu J, Zhao Z, Qiu N, Zhou Q, Wang G, Jiang H, Piao Y, Zhou Z, Tang J, Shen Y, Co-delivery of IOX1 and doxorubicin for antibody-independent cancer chemo-immunotherapy, Nat. Commun, 12 (2021) 2425. [PubMed: 33893275]

[35]. Oh JM, Choi SJ, Lee GE, Kim JE, Choy JH, Inorganic metal hydroxide nanoparticles for targeted cellular uptake through clathrin-mediated endocytosis, Chemistry, an Asian journal, 4 (2009) 67–73. [PubMed: 18988236]

[36]. Wong HL, Bendayan R, Rauth AM, Xue HY, Babakhanian K, Wu XY, A mechanistic study of enhanced doxorubicin uptake and retention in multidrug resistant breast cancer cells using a polymer-lipid hybrid nanoparticle system, J. Pharmacol. Exp. Ther, 317 (2006) 1372–1381. [PubMed: 16547167]

[37]. Li Y, Gao L, Tan X, Li F, Zhao M, Peng S, Lipid rafts-mediated endocytosis and physiology-based cell membrane traffic models of doxorubicin liposomes, Biochim Biophys Acta, 1858 (2016) 1801–1811. [PubMed: 27117641]

[38]. Tesniere A, Schlemmer F, Boige V, Kepp O, Martins I, Ghiringhelli F, Aymeric L, Michaud M, Apetoh L, Barault L, Mendiboure J, Pignon JP, Jooste V, van Endert P, Ducreux M, Zitvogel L, Piard F, Kroemer G, Immunogenic death of colon cancer cells treated with oxaliplatin, Oncogene, 29 (2010) 482–491. [PubMed: 19881547]

[39]. Liu P, Zhao L, Pol J, Levesque S, Petrazzuolo A, Pfirschke C, Engblom C, Rickelt S, Yamazaki T, Iribarren K, Senovilla L, Bezu L, Vacchelli E, Sica V, Melis A, Martin T, Xia L, Yang H, Li Q, Chen J, Durand S, Aprahamian F, Lefevre D, Broutin S, Paci A, Bongers A, Minard-Colin V, Tartour E, Zitvogel L, Apetoh L, Ma Y, Pittet MJ, Kepp O, Kroemer G, Crizotinib-induced immunogenic cell death in non-small cell lung cancer, Nat. Commun, 10 (2019) 1486. [PubMed: 30940805]

[40]. Xu Y, Villalona-Calero MA, Irinotecan: mechanisms of tumor resistance and novel strategies for modulating its activity, Ann. Oncol, 13 (2002) 1841–1851. [PubMed: 12453851]

[41]. Kawato Y, Aonuma M, Hirota Y, Kuga H, Sato K, Intracellular roles of SN-38, a metabolite of the camptothecin derivative CPT-11, in the antitumor effect of CPT-11, Cancer Res, 51 (1991) 4187–4191. [PubMed: 1651156]

[42]. Thorpe D, Butler R, Sultani M, Vanhoecke B, Stringer A, Irinotecan-Induced Mucositis Is Associated with Goblet Cell Dysregulation and Neural Cell Damage in a Tumour Bearing DA Rat Model, Pathol. Oncol. Res., 26 (2020) 955–965. [PubMed: 30919275]

[43]. van der Velden WJ, Herbers AH, Bruggemann RJ, Feuth T, Peter Donnelly J, Blijlevens NM, Citrulline and albumin as biomarkers for gastrointestinal mucositis in recipients of hematopoietic SCT, Bone Marrow Transplant, 48 (2013) 977–981. [PubMed: 23334276]

[44]. de Koning BA, Sluis M, Lindenbergh-Kortleve DJ, Velcich A, Pieters R, Buller HA, Einerhand AW, Renes IB, Methotrexate-induced mucositis in mucin 2-deficient mice, J. Cell. Physiol, 210 (2007) 144–152. [PubMed: 16998802]

[45]. Stringer AM, Gibson RJ, Logan RM, Bowen JM, Yeoh AS, Hamilton J, Keefe DM, Gastrointestinal microflora and mucins may play a critical role in the development of 5-Fluorouracil-induced gastrointestinal mucositis, Exp. Biol. Med. (Maywood), 234 (2009) 430–441. [PubMed: 19176868]

[46]. Wang Y, Probin V, Zhou D, Cancer therapy-induced residual bone marrow injury-Mechanisms of induction and implication for therapy, Curr. Cancer Ther. Rev., 2 (2006) 271–279. [PubMed: 19936034]

[47]. Gamcsik MP, Kasibhatla MS, Teeter SD, Colvin OM, Glutathione levels in human tumors, Biomarkers : biochemical indicators of exposure, response, and susceptibility to chemicals, 17 (2012) 671–691. [PubMed: 22900535]

[48]. Han H, Wang H, Chen Y, Li Z, Wang Y, Jin Q, Ji J, Theranostic reduction-sensitive gemcitabine prodrug micelles for near-infrared imaging and pancreatic cancer therapy, Nanoscale, 8 (2016) 283–291. [PubMed: 26608864]

[49]. Drummond DC, Noble CO, Guo Z, Hong K, Park JW, Kirpotin DB, Development of a highly active nanoliposomal irinotecan using a novel intraliposomal stabilization strategy, Cancer research, 66 (2006) 3271–3277. [PubMed: 16540680]

[50]. Liu X, Jiang J, Chan R, Ji Y, Lu J, Liao YP, Okene M, Lin J, Lin P, Chang CH, Wang X, Tang I, Zheng E, Qiu W, Wainberg ZA, Nel AE, Meng H, Improved Efficacy and Reduced Toxicity Using a Custom-Designed Irinotecan-Delivering Silicasome for Orthotopic Colon Cancer, ACS nano, 13 (2019) 38–53. [PubMed: 30525443]

[51]. Ohtsuka K, Inoue S, Kameyama M, Kanetoshi A, Fujimoto T, Takaoka K, Araya Y, Shida A, Intracellular conversion of irinotecan to its active form, SN-38, by native carboxylesterase in human non-small cell lung cancer, Lung Cancer, 41 (2003) 187–198. [PubMed: 12871782]

[52]. Guichard S, Terret C, Hennebelle I, Lochon I, Chevreau P, Fretigny E, Selves J, Chatelut E, Bugat R, Canal P, CPT-11 converting carboxylesterase and topoisomerase activities in tumour and normal colon and liver tissues, British journal of cancer, 80 (1999) 364–370. [PubMed: 10408839]

[53]. Shingyoji M, Takiguchi Y, Watanabe-Uruma R, Asaka-Amano Y, Matsubara H, Kurosu K, Kasahara Y, Tanabe N, Tatsumi K, Kuriyama T, In vitro conversion of irinotecan to SN-38 in human plasma, Cancer Sci, 95 (2004) 537–540. [PubMed: 15182436]

[54]. Chen Q, Wang C, Zhang X, Chen G, Hu Q, Li H, Wang J, Wen D, Zhang Y, Lu Y, Yang G, Jiang C, Wang J, Dotti G, Gu Z, In situ sprayed bioresponsive immunotherapeutic gel for post-surgical cancer treatment, Nat. Nanotechnol., 14 (2019) 89–97. [PubMed: 30531990]

[55]. Galluzzi L, Buque A, Kepp O, Zitvogel L, Kroemer G, Immunogenic cell death in cancer and infectious disease, Nat. Rev. Immunol, 17 (2017) 97–111. [PubMed: 27748397]

[56]. Galon J, Bruni D, Approaches to treat immune hot, altered and cold tumours with combination immunotherapies, Nat. Rev. Drug Discov, 18 (2019) 197–218. [PubMed: 30610226]

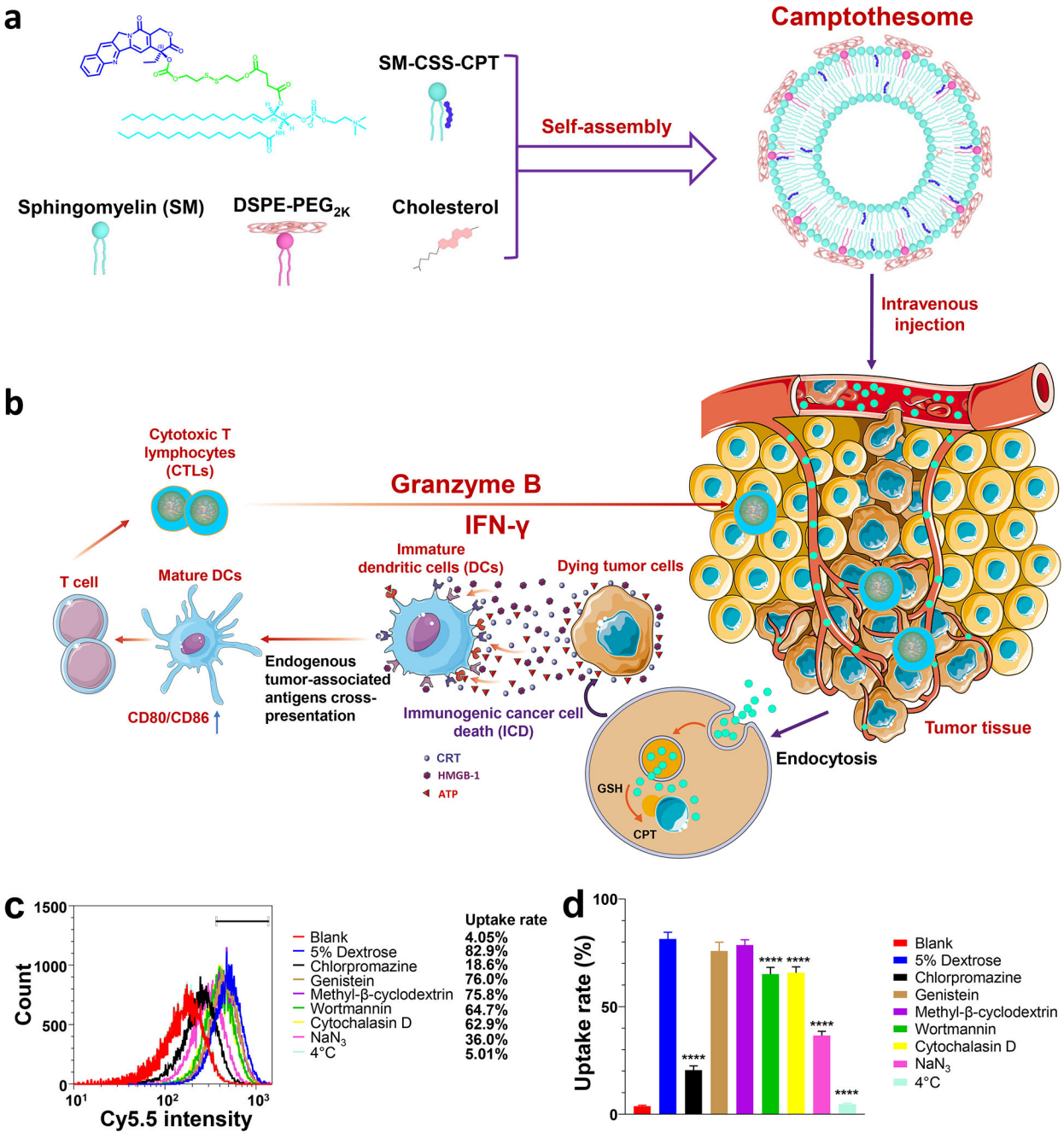

Fig. 1. The self-assembly process, antitumor immune responses, and endocytotic pathway evaluation of Camptothesome.

(**a**) Camptothesome formed by Sphingomyelin (SM), SM-CSS-CPT conjugate[22], DSPE-PEG_{2K} and cholesterol. (**b**) The antitumor immunity triggered by Camptothesome through eliciting immunogenic cell death (ICD). (**c,d**) The effects of endocytotic inhibitors on the cellular uptake of Cy5.5-labeled Camptothesome in CT26 cells through measuring the Cy5.5 intensity using flow cytometry. CT26 cells were pretreated with various endocytotic inhibitors for 0.5 h then incubated with Cy5.5/Camptothesome (50 μg CPT/mL) in the presence of the inhibitors for additional 2 h. (**c**) Representative flow

cytometry histograms of Cy5.5/Camptothesome. (**d**) Cellular uptake percentage rate of Cy5.5/Camptothesome analyzed by flow cytometry. Data in **d** is expressed as mean ± s.d. (n = 3). Statistical significance was determined by one-way ANOVA followed by Tukey's multiple comparisons test. ****P < 0.0001 *vs* 5% Dextrose.

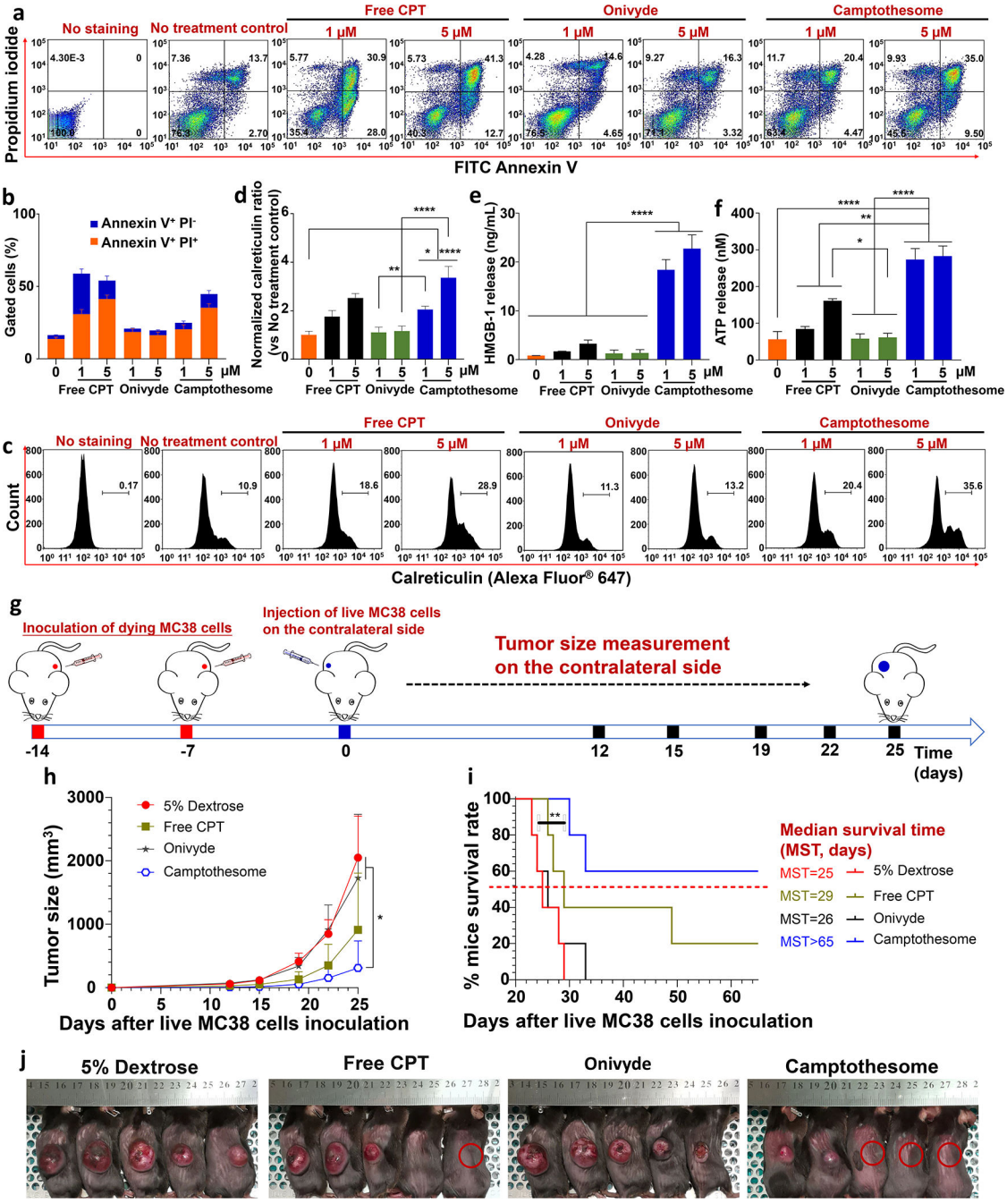

Fig. 2. Camptothesome elicits robust ICD response in CRC.

(**a**) Flow cytometry determination of the apoptotic and necrotic MC38 cells by FITC Annexin V and propidium iodide (PI) after 20 h of treatment with free CPT, Onivyde and Camptothesome at 1 μM or 5 μM of equivalent CPT, respectively. (**b**) Frequency of early apoptotic (Annexin V^+ PI^-) and necrotic/late apoptotic (Annexin V^+ PI^+) MC38 cells. (**c**) Flow cytometry of the calreticulin expression on MC38 cells induced by free CPT, Onivyde or Camptothesome for 20 h at 1 μM or 5 μM of equivalent CPT, respectively. (**d**) Normalized calreticulin expression ratio as compared to no treatment control. (**e**, **f**)

The released HMGB-1 (**e**) and ATP (**f**) concentrations in the medium of samples in (**c**), respectively. Data are expressed as mean ± s.d. (n = 3). (**g-i**) Vaccination approach to validate the ICD potential of Camptothesome *in vivo*. (**g**) Cartoon to show that mice received 2 times (one week apart) of subcutaneous injections of dying MC38 cells (1×10^6) induced by free CPT, Onivyde or Camptothesome at 5 μM of equivalent CPT for 20 h. On day 0, Mice were inoculated with live MC38 cells subcutaneously on the contralateral flank and tumor development was monitored as indicated. (**h**) Tumor growth curves to show the MC38 tumors developed on the contralateral side. Data are expressed as mean ± s.d. (n = 5). (**i**) Kaplan-Meier survival curves. (**j**) Tumor-bearing mice images were taken on day 25. Red circle: tumor-free mouse. Statistical significance was determined by one-way ANOVA followed by Tukey's multiple comparisons test; survival curves were compared by the log-rank Mantel–Cox test. *P < 0.05, **P < 0.01, ****P < 0.0001. *(For interpretation of the references to colour in this figure legend, the reader is referred to the web version of this article.)*

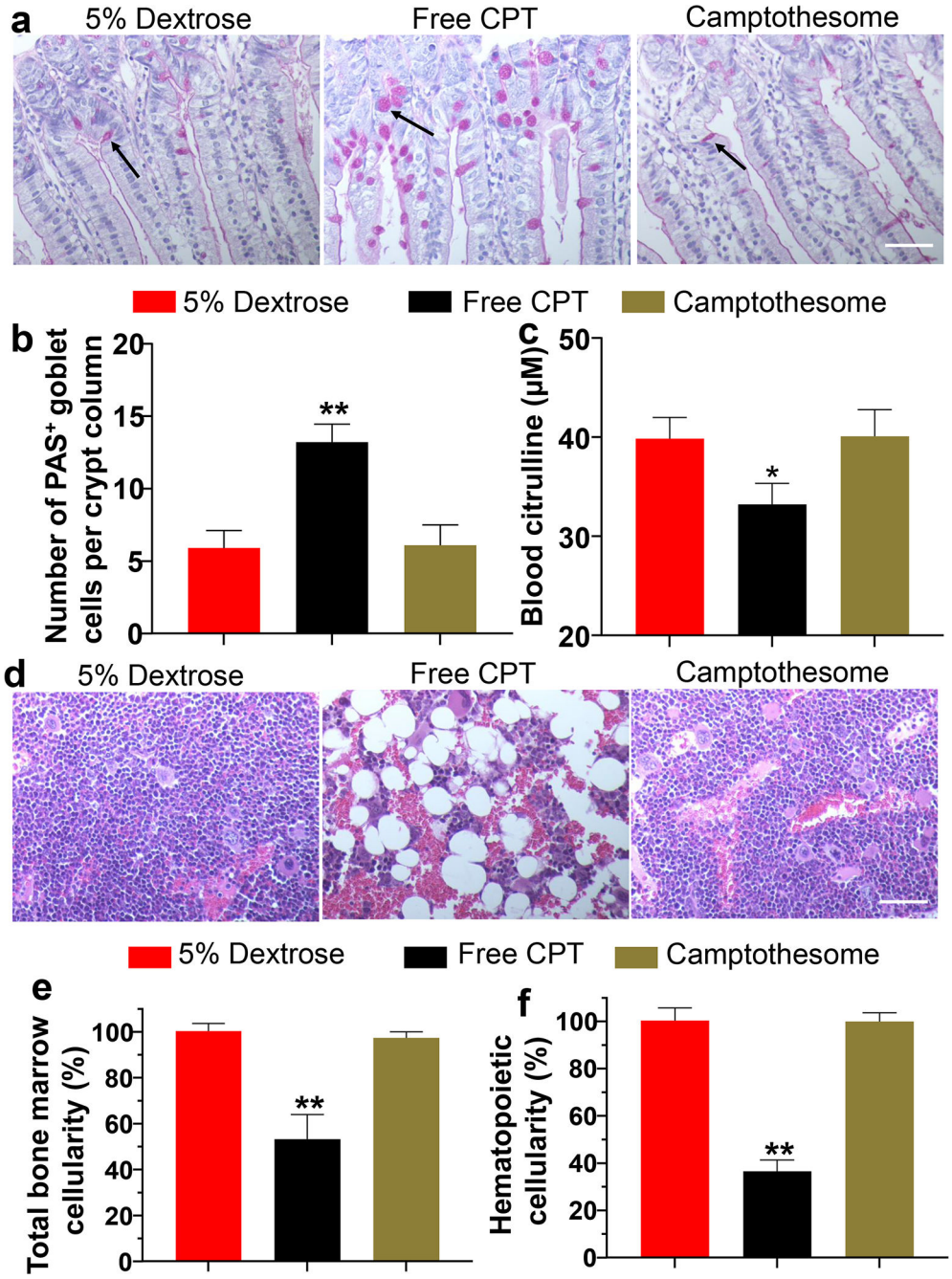

Fig. 3. Diminishing the gastrointestinal (GI) mucositis and bone marrow toxicities.

(**a**) Representative photomicrographs of histologic sections of the intestinal mucosa. Sections were stained by the periodic acid-Schiff (PAS) reaction and counterstained with haematoxylin in Balb/c mice (n = 3) 7 days after receiving MTD of CPT (5 mg/kg) or Camptothesome (30 mg CPT /kg) intravenously. Back arrow indicates the PAS^+ mucin-containing goblet cells[42]; Scale bar: 100 μm. (**b**) Number of PAS^+ mucin-containing goblet cells per crypt column. (**c**) Blood citrulline levels. (**d**) Representative H&E staining images of the sternums from the mice in (**a**). Scale bar: 100 μm. (**e**) Normalized total bone marrow cellularity by measuring the surface area occupied by all cell types in the

sternums[27] and (**f**) Normalized nucleated hematopoietic cells by determining the surface area occupied by nucleated hematopoietic cells[27] from the sternums. Data in **b**, **c**, **e**, and **f** are expressed as mean ± s.d. Statistical significance was determined by one-way ANOVA followed by Tukey's multiple comparisons test. *P < 0.05, **P < 0.01 *vs* 5% Dextrose.

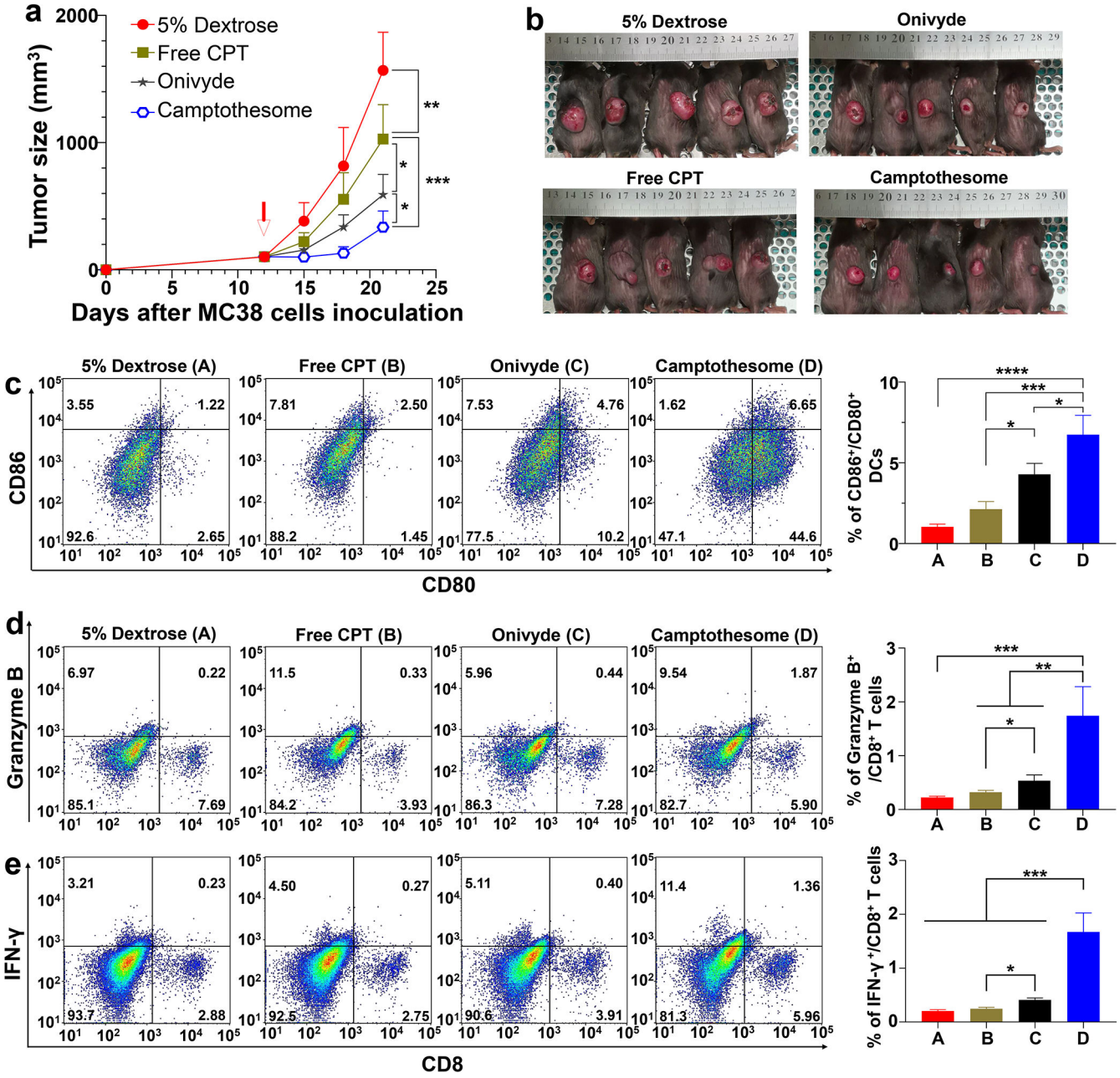

Fig. 4. Camptothesome beats Onivyde on anti-CRC efficacy and immune responses.

(**a**) Tumor growth curves in subcutaneous MC38 tumor-bearing mice (tumors: ~100 mm^3) that were intravenously injected once by free CPT, Camptothesome or Onivyde (8.4 mg irinotecan/kg) at equivalent 5 mg CPT/kg (MTD of free CPT) on day 12. 5% Dextrose was vehicle control. Data are presented as mean ± s.d. (n= 5). (**b**) Tumor-bearing mice images were taken on day 21. (**c-e**) Representative flow cytometric plots of intratumoural $CD80^+/CD86^+$ DCs (**c**), Granzyme $B^+/CD8^+$ T cells (**d**), and IFN-$\gamma^+/CD8^+$ T cells (**e**), and respective quantitative analysis (right panel). Data are presented as mean ± s.d. (n= 3, the tumors were randomly chosen from **a** on day 21). Statistical significance was determined by

one-way ANOVA followed by Tukey's multiple comparisons test. *P < 0.05, **P < 0.01, ***P < 0.001, ****P < 0.0001.

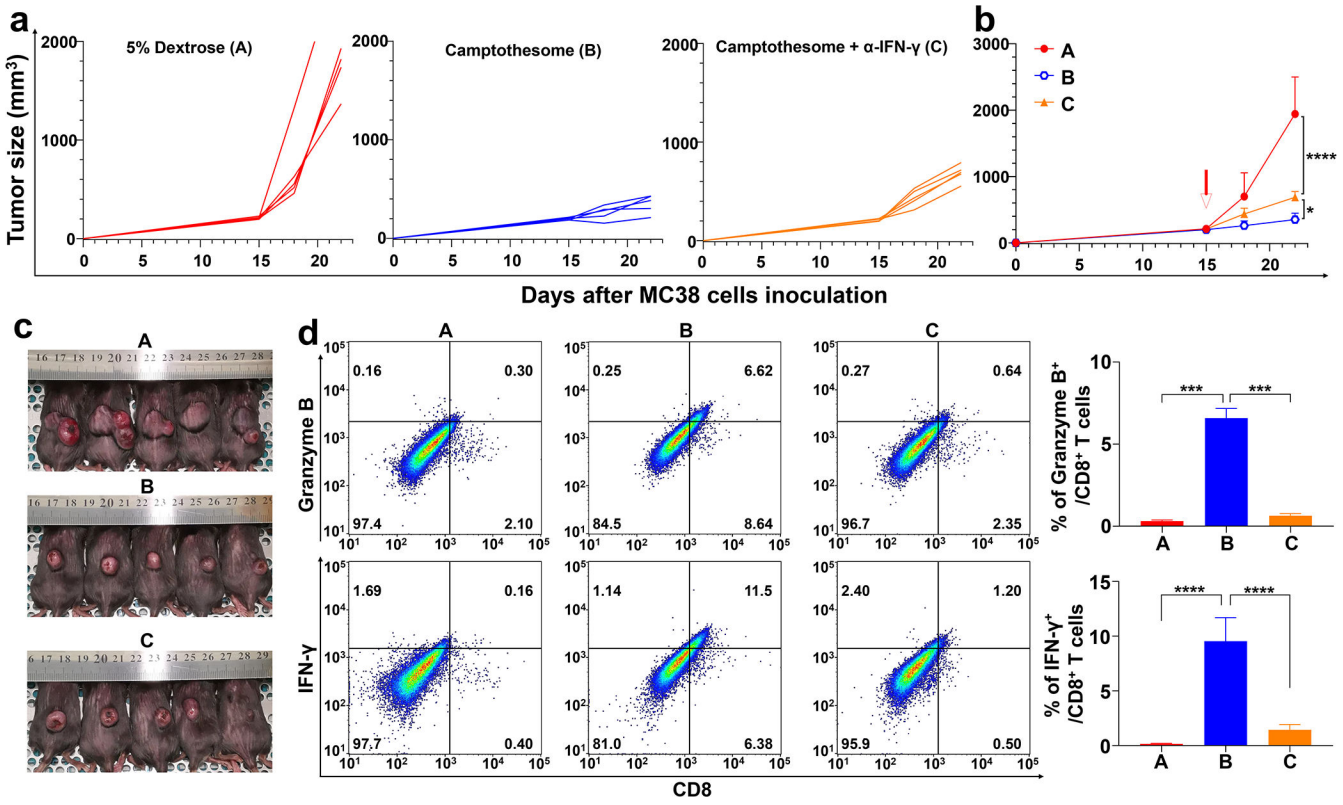

Fig. 5. Therapeutic effects of Camptothesome are partially IFN-γ-dependent.

(**a-c**) Anti-CRC efficacy of Camptothesome in subcutaneous MC38 tumor-bearing mice (tumors: ~200 mm^3). Mice were intravenously injected once with Camptothesome (20 mg CPT/kg) with or without α-IFN-γ (intraperitoneally, 200 μg/mouse/3 days). (**a**) Individual tumor growth curves. (**b**) Average tumor growth curves. Data are expressed as mean ± s.d. (n = 5). (**c**) Tumor-bearing mice images from **b** were taken on day 22. (**d**) Representative flow cytometric plots of granzyme $B^+/CD8^+$ T cells (upper panel) or IFN-$\gamma^+/CD8^+$ T cells (lower panel), and respective quantitative analysis (right panel). Data are expressed as mean ± s.d. (n = 3, the tumors were randomly chosen from **b** on day 22). Statistical significance was determined by one-way ANOVA followed by Tukey's multiple comparisons test. *P < 0.05, ***P < 0.001, ****P < 0.0001.

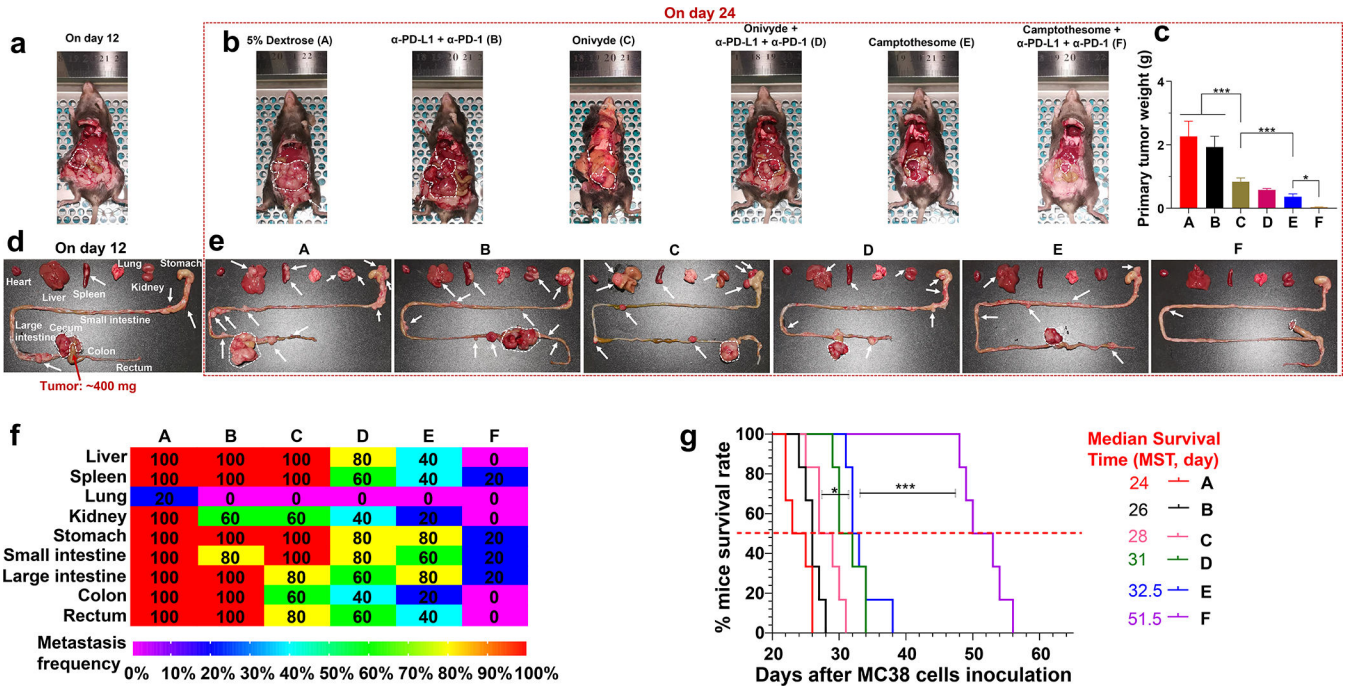

Fig. 6. Fortified therapeutic efficacy in late-stage metastatic orthotopic MC38 model when combined with immune checkpoint blockade.

2×10^6 MC38 cells (DMEM/Matrigel, 3/1, v/v) were inoculated into the cecum subserosa. On day 12, mice (n = 5; tumors: ~400 mg) bearing orthotopic MC38 tumors with noticeable metastasis were intravenously administered once with Camptothesome, or Onivyde (33.6 mg irinotecan/kg) at equivalent 20 mg CPT/kg or their combination with α-PD-L1 + α-PD-1 (intraperitoneally, 100 μg/mouse/3 days, 3 times). (**a-e**) Representative autopsy images (upper panel) and *ex vivo* photograph (lower panel) of the mice before (on day 12, **a,d**) or after (on day 24, **b,e**) the treatments. White dashed circle: big tumor blocks; white arrow: visible tumor metastatic nodules. (**c**) Average orthotopic tumor weight. Data are expressed as mean ± s.d. (**f**) A heatmap showing the tumor metastatic rate. (**g**) Kaplan–Meier survival curves from an independent efficacy study in orthotopic MC38 tumor model (n = 6; tumors: ~400 mg). Survival curves were compared using the log-rank Mantel–Cox test. *P < 0.05, ***P < 0.001.